Biosensors and Bioelectronics 132 (2019) 47–54

Contents lists available at ScienceDirect

Biosensors and Bioelectronics

journal homepage: www.elsevier.com/locate/bios

Graphically encoded suspension array for multiplex immunoassay and quantification of autoimmune biomarkers in patient sera

Kexiao Zheng[a,1], Chao Chen[a,1], Xiuli Chen[b], Menghong Xu[a], Linqi Chen[b], Yining Hu[c], Yanan Bai[d], Binghuan Liu[a], Cheng Yan[a], Hong Wang[d], Jiong Li[a,*]

[a] Nano-Bio-Chem Centre and Key Laboratory for Nano-Bio Interface Research, Suzhou Institute of Nano-tech and Nano-bionics, Chinese Academy of Sciences, Suzhou 215123, China
[b] Department of Pediatric Endocrinology, Genetics and Metabolism, Soochow University Affiliated Children's Hospital, Suzhou 215003, China
[c] Key Laboratory of Computer Network and Information Integration (Southeast University), Ministry of Education and School of Computer Science and Engineering, Southeast University, Nanjing 210096, China
[d] Nano-Devices and Materials Division, Suzhou Institute of Nano-tech and Nano-bionics, Chinese Academy of Sciences, Suzhou 215123, China

ARTICLE INFO

Keywords:
Multiplex immunoassay
Suspension array
Graphical encoding
Cytokines
Autoimmune diabetes

ABSTRACT

In precision medicine, clinical decisions and pharmaceutical evaluations tends to be made upon parallel analysis of multiple protein biomarkers. Currently, the growing needs of high-throughput multiplex immunoassay is partially satisfied by spectrally encoded bead flow suspension arrays and other platforms, yet there is still room for progress in terms of encoding capacity, decoding accuracy, ease-of-manufacture/operation, and cost-effectiveness, for which graphical suspension arrays could make substantial contributions. Here we described a suspension array system made up of graphically encoded silica particles, an automated microplate imager and an in-house data processing program. The micro-fabricated, highly uniform planar particles provide a code space of 128-plex with further extendibility. The derived multiplex immunoassay reaches sub-picogram per milliliter sensitivity level (lowest LoD = 80 fg/ml) with wide dynamic range, as well as high precision and accuracy. The potential of clinical diagnostics was demonstrated by parallel measurement of three serum biomarkers for type 1 diabetes patients. Importantly, use of standard microplates as assay vessel extends its power to high-throughput applications, such as disease screening or drug discovery.

1. Introduction

Accurate and parallel quantification of multiple protein analytes in many specimens during a single test has been long desired as a powerful tool for advancing modern diagnostics, drug development, and personalized medicine (Brody et al., 2010; Kingsmore, 2006). As the number of protein biomarkers for clinical and pharmaceutical applications reaches hundreds (Deyati et al., 2013; Zhao et al., 2015), the need for suitable antibody-based multiplex immunoassay platforms rises high in recent years (Tighe et al., 2015). Hence, numerous innovations from academic and industrial sectors have been devoted to meet the demand. Current approaches have adopted a variety of materials, encoding strategies, and signaling entities, such as bead-based flow-cytometry (xMAP technology by Luminex Corp.) (Fu et al., 2010), DNA-barcodes (Stoeva et al., 2006), molecular beacons (Hu et al., 2015), microfluidics (Fan et al., 2008), chemiluminescence microarrays (Zong et al., 2012), colloidal crystals (Zhao et al., 2008), nanomaterials (Hu et al., 2010), hydrogel stop-flow lithography (Appleyard et al., 2011), and surface plasmonics (Zhang et al., 2014), etc.

As one of the most widely-used multiplex technologies, xMAP and alike platforms (Houser, 2012) take the format of spectral-coded bead flow suspension array, which provides combined advantages of code capacity, throughput scalability, assay sensitivity, panel flexibility, as well as ease-of-automation (Leng et al., 2015), despite the price paid for dealing with flow-beads system's intrinsic difficulties including manufacture variations, insufficient code distance, coding/assay signal crosstalk, non-specific adsorption to hydrophobic beads, long read-out time per sample, fluidics maintenance, and inability to re-reading (Ellington et al., 2010; Leng et al., 2015; Mathur and Kelso, 2010; Waterboer et al., 2006). Improvements to the bead-based suspension array have been continuously proposed (He et al., 2016; Kim et al., 2011; Zhang et al., 2011); however, they do not come free of

* Corresponding author.
E-mail address: jli2006@sinano.ac.cn (J. Li).
[1] These authors contributed equally to this work.

https://doi.org/10.1016/j.bios.2019.02.030
Received 12 October 2018; Received in revised form 25 January 2019; Accepted 4 February 2019
Available online 23 February 2019
0956-5663/

performance compromises, extra technical complexity and/or expenses.

Graphics is another popular code system for suspension arrays, which uses a set of visually distinguishable patterns such as embedded barcodes (Dejneka et al., 2003; Pregibon et al., 2007) or physical shapes (He et al., 2007) to identify different assay particles. Being particle-based like the xMAP system, graphical suspension array is a pseudo-homogenous assay with near-solution diffusion kinetics, resulting in higher mixing efficiency (Yamanishi et al., 2015). Importantly, graph-coded particles own distinctive features that may overcome the drawbacks of color-coded beads, such as better particle shape / size uniformity, digital vs. analog decoding process, and larger flexibility of choosing materials with different chemical, mechanical and/or optical properties for tailor-made microparticles.

To date, most proposed graphical suspension arrays focus on multiplex detection of nucleic acids, with fewer efforts devoted for immunoassay of protein analytes, partially because of complicated assay development issues (analyte fragility, reagent reproducibility, non-specific binding, etc.) (Le Goff et al., 2015). Examination of existing publications in this field shows that only a handful of works presented feasible methodologies with protein assay LoD at 1 pg/ml level or better, notably the stop-flow lithography synthesized barcoded PEG microparticles (Appleyard et al., 2011), and the Evaluation platform based on graphical encoded silicon micro-discs in microfluidic assay cartridges (Falconnet et al., 2015). The superior sensitivity owes thanks to the fast binding kinetics brought by the pressurized microfluidic modalities chosen by both groups for assay vessel. Nonetheless, compared to conventional microplates, the sample throughput of such devices is small due to the limited number of fluidic channels per device, and handling of biomedical samples such as serum and plasma within the microchannels remains another challenge yet to be addressed. Besides, customized opto-microfluidic instrumentation is required to accommodate the above systems.

Herein, we presented a graphically recognizable array of suspension particles ("GRASP") for microplate-format multiplex sandwich immunoassays. The silica-based microparticles are precisely fabricated via lithographic processes and offering a 128-plex coding space. The assay reactions take place in the microplate wells and the readout images are automatically acquired by a commercial microplate imager and processed by a homemade software program to obtain assay results.

2. Materials and methods

2.1. Design of GRASP particles and its coding scheme

The basic structure of the presented suspension particles is a 25 × 14 μm planar silica substrate, with high-reflection optical coatings dotted on its surface at specific positions, forming a 2-dimensional (2D) barcode. On the substrate, the coding elements is a 2 × 4 grid (Fig. 1A). Of the 8 nodes, seven regular ones (3 × 3 μm) are coding nodes constituting a 7-bit string, while the larger one (5 × 4 μm) is a fixed alignment marker to aid machine visual recognition. At each coding node, the presence of a high-reflection thin film coating dot would be visible under an optical microscope to make bit 1, otherwise, absence of the dot would make bit 0. For fluorescence signal readout, the dotted area is excluded from pixel extraction since the high-reflection coating may interfere with the fluorescence.

The thin film coating is made of a periodic multilayer stack of alternating high- and low- refractive index dielectric materials (Si_3N_4 and SiO_2). The thickness of each layer is fine-tuned (Fig. S1A) to reflect broadband incident light at very high efficiency (above 90% reflectance at reference wavelength) via constructive interference. During the imaging step of our assay, the illuminating light transmits through the transparent SiO_2 substrate with little loss, but is strongly reflected at the dot regions, showing a dark pattern on the transmission image of the particle, which is used to mark the particle's identification. The detailed structure of the multilayer stack can be found in Fig. S1B.

2.2. Assay protocols

The workflow of GRASP immunoassay is summarized in Fig. 1A. Essentially, it is adapted from the standard sandwich ELISA protocol, with the replacement of absorbance signal to fluorescence image. First, the suspension array is prepared by mixing the required GRASP particles with different code/capture antibody combinations (one for each analyte) in a Protein LoBind microtube. Add ~500 GRASP particles per code per well to a 96-well filter plate. Next, add 100 μl sample fluid to each well. Place the filter plate on a microplate shaker and agitate the suspension at 700 rpm for 1.5 h at R.T. After incubation, vacuum-wash the filter plate using a microplate washer (BioTek 405 LS) with proper wash solution (such as 1 × PBST, phosphate buffered saline, with 0.5% Tween 20). Next, dispense 100 μl of a prepared cocktail of biotinylated detection antibodies to each well. Incubate the suspension for 30 min at R.T. on a microplate shaker. Vacuum wash the filter plate, then add 100 μl SAPE (streptavidin/R-phycoerythrin conjugate, 0.5 μg/ml) to each well, and react for 30 min at R.T. on a microplate shaker. Vacuum-wash the plate again with an additional final dispense of 150 μl 1 × PBST per well, then transfer the suspension to an assay plate. When the particles are settled at the bottom of wells (usually taking less than 2 min), the plate is ready for image data acquirement. Brightfield and fluorescent images of the above GRASP assay array is obtained automatically using a Cytation 3 multimode microplate imaging reader (BioTek Inc., US) equipped with a 10 × magnification objective, a laser-autofocus, and a 16-bit monochrome CCD (charge coupled device) camera. The instrument is programmed to take 16 non-overlapping photos for both bright field and fluorescent channels at different positions in each well. This ensures adequate number of particles to be collected to yield statistically robust results. Throughout the imaging process, the illumination and exposure settings are kept fixed for quantitative analysis. The large volume of GRASP assay data (3072 raw images from a full 96-well plate, total file size exceeds 5 gigabytes) demands a computational solution. We developed an in-house program to automated data processing (the algorithm and function of which are given in Supplementary material).

In the above protocol, all three rounds of incubation time is set as a normal ELISA (enzyme ligand immunosorbent assay). We also tried a “fast mode” protocol, in which the incubation duration with sample and detection antibodies are set to 30 min, 20 min and 10 min, shortening the total incubation time from 2.5 h to 1 h.

3. Results

3.1. Validation of GRASP immunoassay system

The presented GRASP multiplex assay is an integrated system consists of microfabricated/biochemical reagents, imaging instrument and data processing software. Thus, before running actual bioassays, we conducted thorough validations of each components to examine if the key quality attributes such as fabrication precision, immobilization chemistry, and decoding accuracy, could work properly and reliably.

Photolithography technique is ideal for producing large quantities of micro objects with exact shape and size in batch manner. Through process optimization, we have achieved < 10% relative X-Y tolerance, which is satisfactory at feature size close to 1 μm and the particles have excellent physical uniformity (Fig. S2A). Notably, the high particle yield (30 million particles per 6-in. wafer) effectively reduces the unit expense.

Precise control of material deposition (Fig. S2B) is crucial for our application, because the quality of the high-reflection thin film determines the optical contrast of the coding dots, which eventually affects the decoding accuracy. Microscope images by a color camera show that the microfabricated GRASP coding dots strongly reflect the blue spectrum of the incident light (Fig. 1B, left), making themselves easily recognizable on the transmitted image (Fig. 1B, right). This result is

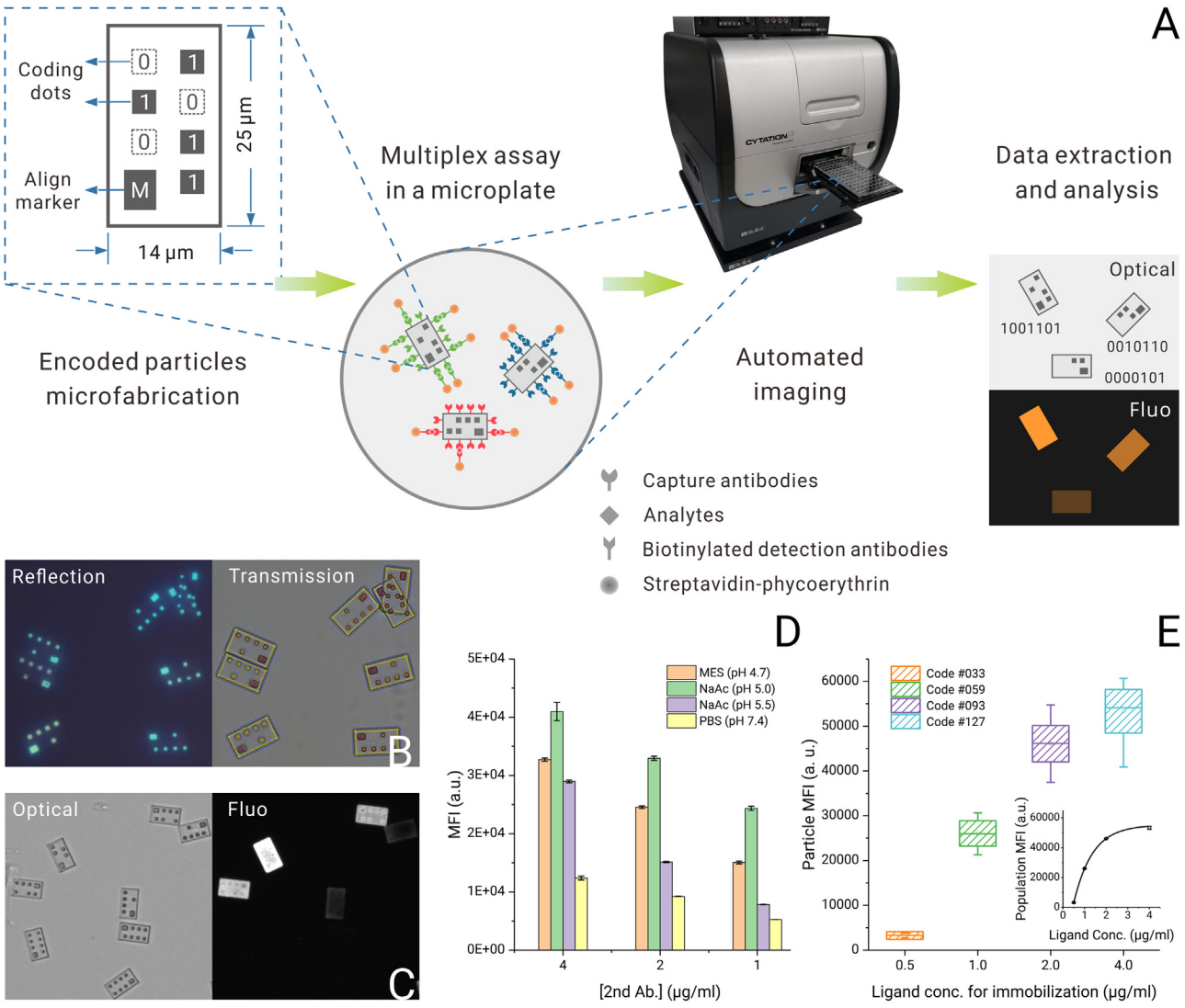

Fig. 1. Scheme and characteristics of the GRASP particles. (A) Layout of the high-reflection thin film coding matrix on particle surface and key steps of multiplex immunoassay workflow based on the GRASP suspension array. (B) Reflection (left) and transmission (right) image images of unmodified particles taken by a color camera. (C) Brightfield (left) and fluorescent (right) images of mixed particles with different fluorescence intensity taken by a monochrome camera. (D) Mean fluorescent intensity (MFI) of DAylight 488-conjugated goat-anti-mouse IgG binding to particles immobilized with mouse-anti-human IFNγ via EDC/NHC chemistry proceeded in four different buffers. (E) MFI distribution by code of mixed particles immobilized with 0.5 (Code #033), 1.0 (Code #059), 2.0 (Code #093), and 4.0 (Code #127) μg/ml, respectively. Insert: asymptotic fitting of population MFI (n = 3) against ligand concentration, R^2 = 0.999998.

consistent with our thin film reflectance simulation results (Fig. S1A).

An efficient, yet often overlooked approach of biosensor surface optimization is increasing the density of immobilized capture molecules. In our work, monoclonal capture antibodies are covalently cross-linked to the carboxylic GRASP particle surface (see Supplementary material for details). It is known that favorable buffer pH and composition could facilitate ligand binding via raising the local concentration at the surface. Using a Biacore T200 SPR (surface plasmon resonance) system, we examined the pre-concentration effect of four capture antibodies to a carboxylic surface in six different buffers, and found that the amount of electrostatically attracted antibody varied drastically with the selected coupling buffer (Fig. S3), as sodium acetate (pH 5.0) resulted far better near-surface ligand enrichment than MES buffer (pH 4.7) commonly used for EDC conjugation. Further experiment with antibody immobilized particles in different coupling buffers confirmed that the pre-concentration plays an important role in the antibody loading process (Fig. 1D).

Instrument and software are crucial components for an imaging based assay system since they determine factors such as image acquisition speed, quality, and accuracy of pattern recognition, etc. The Cytation microplate imager we used offers automated, multi-fields microplate image acquisition with a wide fluorescence dynamic range. A representative dual-channel image obtained by the imager is shown in Fig. 1C. Typically, it takes 1.5 h for the imager to shot all the fields required from a fully loaded 96 well plate. The computer program we developed delineates randomly scattered particles and read the graph codes, while automatically excluding artifacts or defections such as debris, overlapping particles, and objects on the edge of the imaging field (Fig. S4). Running on a mainstream PC, it takes less than 10 min for the program to extract and analyze data from a fully loaded 96-well plate.

In a proof-of-principle experiment, we prepared three lots of GRASP particles bearing four different codes, with each code immobilized with a dye-labeled antibody at a fixed concentration (e.g. all three lots of #093 particles were incubated with 1 μg/ml labeled antibodies). Then all four coded particles of the same lot (~ 500 per code) were added to a well and imaged. The results were shown in Fig. 1E. As expected, the program correctly classified four populations of coded particles at

different fluorescent intensity levels. The insert shows the lot average of MFI values of each coded population fitted smoothly to an asymptotic binding model. Importantly, signal CVs (coefficient of variance) for all lots is under 2%, indicating that large number of particles could effectively reduce random error. Further experiments in which fluorescent dye tagged secondary antibody binds to particles underwent conjugation reaction with different amount of input capture antibodies suggest that 10 μg antibody per reaction is an balanced choice between immobilization density and reagent cost, while only slight decrease was observed when input particles increased from about 10^4 to 10^5 per reaction (Fig. S5).

The stability of the antibody-immobilized, ready-to-use GRASP particles has been briefly investigated by comparing the signals of three analytes from assays using the corresponding particles store in 4 °C 1 × PBST after 7 and 42 days of capture antibody coupling, respectively. The data (Fig. S6) shows at day 42, the assay produced 96.8%, 80.6%, and 91.2% signal in relative to that at day 1.

3.2. Multiplex immunoassay performance

To evaluate the bench performances of GRASP array, we use human cytokines and growth factors dissolved in assay buffer as model protein analytes.

Specificity is a critical prerequisite to develop a multiplex assay. Cross-reactivity between different reagents and/or analytes must be minimized, if not eliminated, to avoid false results (Juncker et al., 2014). We examined GRASP array's tolerance for multiplexing by applying single or mixed analytes to the suspension array. The incubation time for capture and detection antibodies are 1.5 h and 0.5 h, respectively. For single analyte (Fig. 2A), all non-target particles produced uniformly small signal readings after incubation with high concentration analytes (0.5 ng/ml), indicating that the simple BSA coating efficiently blocked undesired binding interactions. Next, we prepared three combinations of four analytes at different concentration levels and observed their signal response from GRASP assay. As shown in Fig. 2B, the target signals from each mix are in good accordance with the concentration gradient settings. These experiments proves that the non-specific adsorption of other analytes, detection antibodies or SAPE on the surface of GRASP particles is insignificant; and the specificity of the capture antibodies are well retained.

Next, we established calibration curves for each analyte using pre-mixed standards. Compared to monoplex assays, standards cocktail could benefit a multiplex assay by lowering the number of wells and pipetting operations required to obtain calibration curves by n-fold (n is the number of analytes), thus allow more specimens to be assayed on the same plate. First, we conducted a 4-plex assay with total incubation time of 2.5 h, with calibrator mixes having 11 concentration levels (from 3 ng/ml down to 0.05 pg/ml). Standard logistic regression (4-P) served as the non-linear fitting model. The Limit-of-Detection (LoD) was determined following the guidance established by Clinical and Laboratory Standards Institute (Armbruster and Pry, 2008), which defines $\text{LoD} = \text{mean}_{\text{Blank}} + 1.645 \times \text{SD}_{\text{Blank}} + 1.645 \times \text{SD}_{\text{Lowest}}$ concentration sample (SD is standard deviation). The fitted curves are plotted in Fig. 3A. The CoD R square values close to 1 ($R^2 > 0.992$ for all) and very small p-values of F-test ($p < 5 \times 10^{-8}$ for all) suggest the curves achieved satisfactory goodness-of-fit. All assays achieved 4 logs of dynamic range. The calculated LoDs for human TNFα, IFNγ, IL-1β and FGF-19 are 0.08, 0.21, 0.08, and 0.17 pg/ml.

We also tested an accelerated GRASP workflow (fast mode), which saves an extra of 1.5 h incubation time. This is demonstrated by a 6-plex assay involving GRASP particles against human TNFα, IFNγ, IL-1β, FGF-19, FGF-9, and VEGF (11 concentration levels, serial-diluted from 10 ng/ml down to 1.05 pg/ml). The calibration curves (Fig. 3B) show that most analytes could be quantified at 1 pg/ml and the dynamic range cross 4 logs except FGF-9 ($R^2 > 0.999$ for all). Note that the LoDs are at similar levels to those in Fig. 3A, indicates that increased number of reagents (detection antibodies) did not result in more unspecific adsorption to the particle surface. Single analyte control samples (50 pg/ml) further proved that there is minimal cross-reaction among the six populations of GRASP particles (Fig. S7).

As compared to existing high-sensitive multiplex technologies (Yamanishi et al., 2015; Yeung et al., 2016), the sensitivity performance is satisfactory, considering the fact that the diffusion-driven binding kinetics is relatively slow versus that of homogenous or microfluidic systems. The total time-to-results (start on sample addition) for the two operation modes is approximately 3 h or 4.5 h for a fully loaded 96 well microplate, respectively, including ~30 min hands-on time and 1.5 h imaging.

3.3. Evaluation of assay precision and accuracy

We constructed the precision profile for GRASP assay by repeatedly

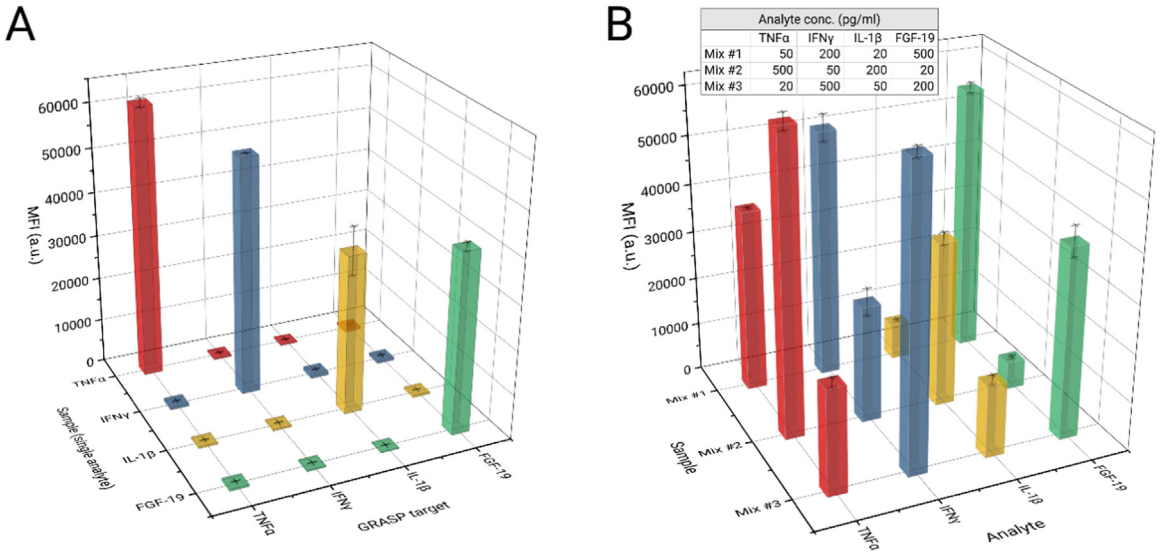

Fig. 2. Specificity of GRASP assay. (A) Signal responses of 4 protein analytes at 0.5 ng/ml when added alone to an array of 4 coded particles against each analyte. (B) Signal responses of three combinations of the four protein analytes (at three different concentration levels) when added together to the same array of particles as in (A).

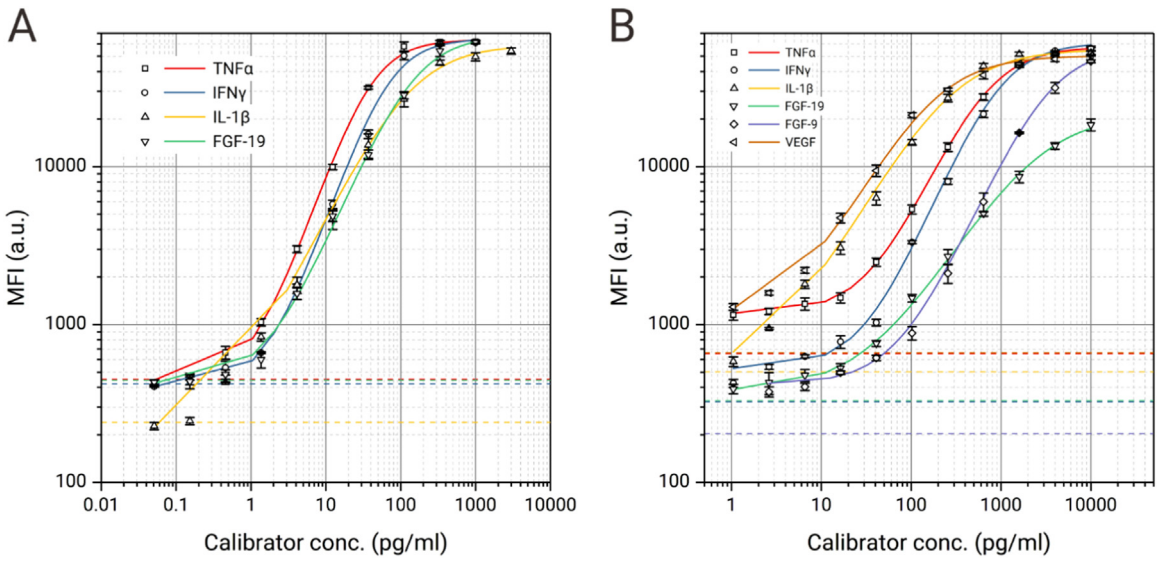

Fig. 3. Plotting of standard curves for a 4-plex (TNFα, IFNγ, IL-1β and FGF-19) GRASP assay with total incubation of 3.5 h (A) and an 6-plex (TNFα, IFNγ, IL-1β, FGF-19, FGF-9, and VEGF) with total incubation of 1.5 h (B). Dashed lines stand for Limit-of-Detection (LoD).

Table 1
Coefficient of variation (CV) values of the back-calculated assay quality control (QC) results from two GRASP assays. Assay #1, a duplex assay for TNFα and IL-1β in buffer, was repeatedly performed in three days (one plate per day, four replicate per plate). The standards ranging from 1600 pg/ml to 2.6 pg/ml. In-house diluted QCs are 533.3 (H), 106.7 (M), and 21.3 (L) pg/ml, respectively. Assay #2, a monoplex assay for GAD_{65} auto-antibody in serum, was repeatedly as in assay #1 (three replicates per plate). The standards ranging from 2000 U/ml to 5 U/ml. In-house diluted QCs are 500 (H), 100 (M), and 25 U/ml, respectively. All standards and QC4 (49.6 U/ml) are from an in-vitro diagnostics provider and pre-calibrated.

			Intra-assay CV			Inter-assay CV
Assay	Analyte		Run #1	Run #2	Run #3	3 runs
#1	TNFα	QC1 (H)	6.3%	11.2%	12.1%	4.3%
		QC2 (M)	3.7%	3.8%	4.0%	2.9%
		QC3 (L)	10.3%	13.0%	7.0%	4.2%
		Mean	**6.8%**	**9.4%**	**7.7%**	**3.8%**
	IL-1β	QC1 (H)	9.8%	3.9%	7.7%	13.6%
		QC2 (M)	9.0%	7.2%	5.1%	7.3%
		QC3 (L)	2.7%	7.5%	4.6%	3.5%
		Mean	**7.2%**	**6.2%**	**5.8%**	**8.1%**
#2	GAD Ab	QC1 (H)	2.2%	1.5%	5.2%	9.5%
		QC2 (M)	6.0%	3.0%	7.6%	1.4%
		QC3 (L)	10.6%	2.8%	7.5%	8.2%
		QC4 (V)	3.6%	3.9%	3.1%	2.5%
		Mean	**5.4%**	**2.8%**	**5.8%**	**5.4%**

performing two assays. The first one is a duplex assay for human TNFα and IL-1β dissolved in buffer. For each analyte, the assay contains eight standards ranging from 1600 pg/ml to 2.6 pg/ml and three quality controls (QC) diluted from the highest standard. All standards and QCs have 4 replicates per plate. The second one is a monoplex assay for human GAD autoantibody in serum. The assay contains six vendor-calibrated standards (RSR Ltd.) ranging from 5 to 2000 U/ml, three in-house diluted QCs and one vendor-calibrated QC. All data points have three replicates per plate. Both assays have been run for three times independently on different days (one plate per day). Using each run's analyte-specific calibration curves (Fig. S8), the concentrations of all QC replicates in the run were back-calculated. The corresponding coefficient of variation (CV) is shown in Table 1. In assay #1, the maximum intra-assay CV recorded for any QC is 13.0% for TNFα and 9.8% for IL-1β, respectively. On average, the intra-assay CV lie between 5.8% and 9.4%; and the inter-assay CV is 3.8% for TNFα and 8.1% for IL-1β. In assay #2, the average intra-assay CV lie between 2.8% and 5.8% (individual maximum is 10.6%), and the average inter-assay CV is 5.4%. Judging by the common acceptance criteria (CV < 15%), the GRASP assay achieves fine intra- and inter-assay precision. The QC recovery values are listed in Table S2. The accuracy for the diluted TNFα, IL-1β QCs are outstanding (mean recovery values come near 100%). However, most recovery data of the diluted anti-GAD QCs in serum failed to enter the common acceptance range (80–120%), which is in sharp contrast to that of the vendor calibrated QC (91.4–96.1%). This is likely to be a manifestation of the matrix effect, indicating that pre-calibrated samples should be first considered when choosing assay controls for serological analytes.

To further assess the effect of sample matrix and dilution on the accuracy of GRASP assay, we conducted two preliminary studies on a triplex assay for human TNFα, IL-1β, and IFNγ. We also performed parallel experiments using a commercial CBA assay (Cytometric Bead Array, a bead-based multiplex immunoassay provided by BD Biosciences) to serve the purpose of inter-platform comparison. Reagents used in both assays are from the CBA kits except for the GRASP particles. In the spike-and-recovery study, the analytes were dissolved separately in buffer, cell culture supernatant and human serum to represent different sample matrices. Each analyte was prepared at three concentration levels: 1000, 150, and 25 pg/ml using lyophilized standards. In the linearity-of-dilution study, control for each analyte at 1000 pg/ml was serially diluted 2-, 4-, and 8-fold using 1× PBST for GRASP assay and kit-provided diluent for CBA assay. The results are summarized in Table 2. For the spiked-in controls, we observed that most samples have recovery value in between or close to the 80–120% range for both GRASP and CBA assay. Exceptions are recorded for IL-1β in serum having recovery below 80%, and for TNFα (QC M and L) in serum which exceeds 120%. The former again indicates inhibitory effect of serum, while the latter may due to interference from non-specific binding serum components with cross-activity to the assay antibodies. For the diluted controls, all linearity-of-dilution values are in between 80% and 120%, yet for serum dilution the CBA assay exhibits better parallelism. We attribute this to a poor matrix matching of the serum samples with the PBST diluent used in the GRASP assay.

3.4. Autoimmune biomarker detection from patient sera

Type 1 diabetes (T1D) is characterized by a patient's insulin-producing β cells of the pancreatic islets being mistakenly attacked by the

Table 2
Test of spike-and-recovery and linearity-of-dilution using multiplex set of TNFα, IFNγ and IL-1β for GRASP assay, with head-to-head comparison to BD Cytometric Bead Array (CBA) assay. (A) Recovery rates of three spike-ins (at 1000, 150 and 25 pg/ml concentrations) in buffer (1× PBST), A549 cell culture supernatant and health human serum. (B) Recovery rates of serial dilutions (2×, 4× and 8×) in the same sample matrices in (A). Diluents used are 1× PBST for GRASP assay, and the kit-provided assay diluent for CBA assay.

Spike-and-Recovery

Sample matrix		Buffer			Cell culture supernatant			Serum		
[Spike-in] (pg/ml)		1000	150	25	1000	150	25	1000	150	25
TNFα	GRASP	96.2%	91.1%	77.8%	96.9%	87.8%	84.8%	77.2%	120.1%	130.8%
	CBA	96.0%	92.2%	75.9%	89.0%	94.0%	80.9%	87.4%	86.3%	83.4%
IFNγ	GRASP	89.4%	98.3%	91.4%	88.3%	105.6%	97.9%	88.3%	84.8%	87.5%
	CBA	100.2%	92.1%	82.0%	93.1%	93.1%	87.3%	85.3%	79.0%	85.3%
IL-1β	GRASP	98.5%	92.8%	78.4%	96.6%	100.2%	125.4%	71.7%	64.9%	53.7%
	CBA	94.1%	84.9%	60.4%	88.5%	94.7%	94.1%	86.9%	84.5%	64.6%
Linearity-of-Dilution										
Sample matrix		Buffer			Cell culture supernatant			Serum		
[Spike-in] (pg/ml)		2×	4×	8×	2×	4×	8×	2×	4×	8×
TNFα	GRASP	97.8%	90.8%	94.9%	92.1%	97.9%	104.8%	100.0%	116.7%	103.2%
	CBA	92.6%	100.4%	96.0%	97.7%	101.2%	100.8%	101.9%	99.0%	91.7%
IFNγ	GRASP	104.5%	90.4%	102.7%	102.8%	98.4%	102.7%	88.1%	105.2%	99.1%
	CBA	89.6%	97.5%	94.8%	93.7%	97.4%	98.8%	102.1%	98.1%	90.8%
IL-1β	GRASP	98.3%	95.9%	94.9%	95.8%	93.6%	103.7%	108.0%	115.1%	88.6%
	CBA	89.6%	97.1%	88.7%	96.3%	97.6%	92.3%	99.6%	93.1%	89.1%

body's own immune system. Immune biomarkers serve as tools for the prediction, progression, and validation of therapeutic responses in T1D (Rekers et al., 2015). Combined measurement of serum autoantibodies recognizing the islet cell antigens glutamic acid decarboxylase (GAD_{65}), insulinoma antigen 2 (IA-2) and Zinc Transporter 8 (ZnT8) could provide 95.5% detection rate for type 1 diabetes, while individual measurement of these autoantibodies gives detection rate of 68%, 72%, and 63%, respectively (Wenzlau et al., 2007). Other studies identified these autoantibodies as prognostic markers for T1D patients received pancreatic transplantation as a potential cure (Piemonti et al., 2013). In current practice the most-widely used detection method for these serum biomarkers is radio-immunoassay (RIA), which is known for its poor performances and cumbersomeness (Zhang et al., 2014). Although enzyme-immunoassay (EIA) and chemiluminescence immunoassay (CLIA) are replacing RIA in recent years, research efforts are continually made in seeking of sensitive and multiplex solutions for T1D auto-antibodies detection (Duan et al., 2017; Zhang et al., 2014).

The sandwich GRASP multiplex assay we constructed for the three T1D autoantibodies mentioned above uses their corresponding recombinant antigens as immobilized capture ligands. To aid quantitative comparison, we used recombinant antigens, detection antibodies, and serum calibrators and controls from a provider of diagnostic T1D ELISA kits (RSR Ltd.) except for recombinant ZnT8 (not available from RSR, purchased from another vendor). Then, we measured the three autoantibodies in serum specimens collected from 27 new-onset T1D patients (13 girls and 11 boys between age 1.1 – 14.1 year), one T2D patient and 8 non-diabetic controls (between age 7.5 – 12.8 year) using both GRASP and ELISA. All serum specimens are diluted using assay diluent from RSR to minimize matrix interference.

From the recovery and CV data of pre-calibrated controls (Table S3), we found both assays had satisfactory precision and accuracy, while in the latter case GRASP performed even better. The fluorescent signal from GRASP assay (Fig. S9) shows that all T1D specimens tested positive (at least one autoimmune antibody is above assay cut-off), while all of the negative controls (T2D and non-diabetic) tested negative (none of the three exceeds assay cut-off), as expected. When the calculated titers are plotted against each other (Fig. 4), we found overall good accordance. The Pearson correlation coefficient for GAD_{65} Ab, IA-2 Ab, and ZnT8 Ab are 0.93, 0.81, and 0.96, respectively. More importantly, as compared to the clinical diagnosis results from the hospital, GRASP assay reaches a sensitivity of 92% and a specificity of 100%, equivalent

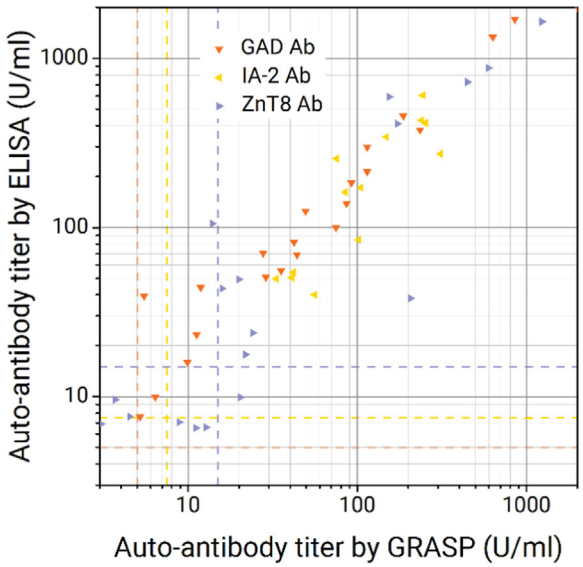

Fig. 4. Scatter plot of three serum autoimmune antibody titers measured by GRASP assay and ELISA. The dash lines stands for positive cut-off values of each auto-antibody (Orange: 5 U/ml for GAD_{65} Ab; Yellow: 7.5 U/ml for IA-2 Ab; Purple: 15 U/ml for ZnT8 Ab). Note that only the quantifiable titers are plotted, sample tested out of assay quantification range are omitted.

to that of ELISA (Table S4). There are only slight difference of the number of positive titers between the two assays.

4. Discussion

In GRASP assay, multiple analytes could be quantified at 1 pg/ml level for a total incubation time of 1 h, and can achieve 0.1 pg/ml sensitivity if extended to 2.5 h. In both cases, the dynamic range spans 4 logs. The sensitivity and dynamic range can be further promoted by improving the particle surface properties and upgrading the camera. That said, the demonstrated performances are superior to those of most ELISA kits and rivals many existing multiplex immunoassays. According to existing knowledge, the typical blood concentration of cytokines are at low pg/ml to sub-pg/ml level, and the abundance variation between patient/non-patient could be 3–4 logs (Brand et al., 2011; Yurkovetsky

et al., 2007). Hence, the quantification capability of the GRASP assay is sufficient in most application scenarios and in accordance with the current expectations for modern immunoassay technologies (Spriggs et al., 2012; Yeung et al., 2016). Importantly, the use of conventional 96 well plates as assay vessel enables high sample throughput, which is often a shortcoming for other proposed multiplex platforms using tailor made vessels such as microfluidic cartridges.

When developing assays for analytes in biological fluids such as serum or plasma using the GRASP system, our study suggests that optimization of assay diluent (e.g. matched matrix) is of critical importance to reduce cross-activity. On the other hand, anti-fouling surface modification / blocking would better inhibit non-specific binding. Moreover, the matrix effect, selectivity, and minimum-required dilution (MRD) should be adequately addressed to ensure assay reliability as like other ligand-binding assays (Tu and Bennett, 2017).

A distinct advantage of GRASP assay is the redundancy of data sampling. The relatively small footprint (compared to some proposed suspension array particles, i.e. 270 × 70 μm for barcoded hydrogel particles (Appleyard et al., 2011) or 40 μm diameter for Evaluation discs (Falconnet et al., 2015)) may facilitate mixing and allows more than 9×10^4 particles (theoretically) to occupy the well bottom area of a standard 96 well microplate. As the microplate well can easily accommodate hundreds of replicate particles for a single analyte, the well-wide result is of considerable statistical sample size and consequently the margin of error could be very small. That is in accord with the overall excellent precision observed in our experiments. Although in practice, limiting factors such as particle overlapping have to be considered when determining redundancy. Our analysis on this issue (see Supplementary Material) reveals that ~35 analytes can be assayed in parallel using a 96 well plate for imaging, and if a 24 well (with larger bottom area) is used then the multiplicity can reach more than 90.

Except for the particles, all hardware and materials required for GRASP assay are off-the-shelf commercial products and ELISA-compatible. The particle microfabrication process could also be readily implemented in any qualified facility. Considering that many proposed multiplex assay systems demand customized and usually complicated instrumentation (Ghodbane et al., 2015; He et al., 2016; Lee et al., 2010), our platform is easier to assemble and implement. Leveraging the mass production power from the semiconductor industry, the particle manufacture process adds vanishingly small amount to the unit test cost of the assay (one analyte per well, estimated roughly one USD, calculation listed in Supplementary material).

The multiplex extendibility of the GRASP assay (10–100 analytes) would potentially enable it to enter the area of affinity-based proteomics, which is now dominated by antibody microarrays (Ayoglu et al., 2011) and other suspension array platforms (Krishnan et al., 2018). Given proper optimization and validation (cross-activity and parallelism in particular), we foresee that it may found niche applications having special emphasize on quantification ability, sample throughput and assay speed, such as biomarker research and clinical proteomic profiling.

The GRASP array can serve as a general-purpose multiplex platform by tethering other capture modalities such as DNA probes, aptamers or nanobodies, thanks to the rich chemistry for silica surface conjugation (Vansant et al., 1995). The ability of multiplex nucleic acid (microRNAs and HPV genes) detection has been demonstrated in our previous works (Jiang et al., 2014; Xu et al., 2017).

5. Conclusions

In summary, the GRASP suspension array we developed in this study provides a large coding space, high-throughput capacity, and overall analytical performances competitive to most multiplex assays, with simple assay construction and workflow. Its potential use as a diagnostic tool has been demonstrated by measuring three diabetic biomarkers in clinical specimens. Although the acclaimed next generation ligand-binding assay is emerging (Mora et al., 2014), multiplex platforms without dedicated hardware setup and special training requirements such as the GRASP system would prove valuable where operational compatibility, assay throughput and/or cost are concerned.

CRediT authorship contribution statement

Kexiao Zheng: Formal analysis, Funding acquisition, Investigation, Methodology, Project administration, Validation, Visualization, Writing - original draft, Writing - review & editing. **Chao Chen:** Investigation, Validation, Writing - review & editing. **Xiuli Chen:** Investigation, Resources, Validation. **Menghong Xu:** Investigation. **Linqi Chen:** Funding acquisition, Resources. **Yining Hu:** Data curation, Formal analysis, Methodology, Software. **Yanan Bai:** Investigation. **Binghuan Liu:** Investigation. **Cheng Yan:** Investigation. **Hong Wang:** Investigation. **Jiong Li:** Conceptualization, Funding acquisition, Methodology, Project administration, Supervision, Writing - original draft.

Acknowledgments

We are grateful for the financial support from National Natural Science Foundation of China (Project nos. 31300817 and 61671445), Instrument Developing Project of CAS (Project no. YZ201652), Jiangsu Provincial Science and Technology Department (Project no. BE2016681), and Suzhou Municipal Bureau of Health (Project no. LCZX201407). We also thank Yiqun Wang for his aid in photolithography, Li Jiang for her aid in Biacore measurements, and Dr. Kefeng Pu for his aid in cell culture.

Declaration of interests

None.

Appendix A. Supplementary material

Supplementary data associated with this article can be found in the online version at doi:10.1016/j.bios.2019.02.030.

References

Appleyard, D.C., Chapin, S.C., Doyle, P.S., 2011. Multiplexed protein quantification with barcoded hydrogel microparticles. Anal. Chem. 83 (1), 193–199.
Armbruster, D.A., Pry, T., 2008. Limit of blank, limit of detection and limit of quantitation. Clin. Biochem. Rev. 29 (Suppl 1), S49–S52.
Ayoglu, B., Häggmark, A., Neiman, M., Igel, U., Uhlén, M., Schwenk, J.M., Nilsson, P., 2011. Systematic antibody and antigen-based proteomic profiling with microarrays. Expert Rev. Mol. Diagn. 11 (2), 219–234.
Brand, R.E., Nolen, B.M., Zeh, H.J., Allen, P.J., Eloubeidi, M.A., Goldberg, M., Elton, E., Arnoletti, J.P., Christein, J.D., Vickers, S.M., Langmead, C.J., Landsittel, D.P., Whitcomb, D.C., Grizzle, W.E., Lokshin, A.E., 2011. Serum biomarker panels for the detection of pancreatic cancer. Clin. Cancer Res. 17 (4), 805–816.
Brody, E.N., Gold, L., Lawn, R.M., Walker, J.J., Zichi, D., 2010. High-content affinity-based proteomics: unlocking protein biomarker discovery. Expert Rev. Mol. Diagn. 10 (8), 1013–1022.
Dejneka, M.J., Streltsov, A., Pal, S., Frutos, A.G., Powell, C.L., Yost, K., Yuen, P.K., Müller, U., Lahiri, J., 2003. Rare earth-doped glass microbarcodes. Proc. Natl. Acad. Sci. USA 100 (2), 389–393.
Deyati, A., Younesi, E., Hofmann-Apitius, M., Novac, N., 2013. Challenges and opportunities for oncology biomarker discovery. Drug Discov. Today 18 (13–14), 614–624.
Duan, K., Ghosh, G., Lo, J.F., 2017. Optimizing multiplexed detections of diabetes antibodies via quantitative microfluidic droplet array. Small 13 (46), 1702323.
Ellington, A.A., Kullo, I.J., Bailey, K.R., Klee, G.G., 2010. Antibody-BAsed Protein Multiplex Platforms: Technical and Operational Challenges. Clin. Chem. 56 (2), 186–193.
Falconnet, D., She, J., Tornay, R., Leimgruber, E., Bernasconi, D., Lagopoulos, L., Renaud, P., Demierre, N., van den Bogaard, P., 2015. Rapid, sensitive and real-time multiplexing platform for the analysis of protein and nucleic-acid biomarkers. Anal. Chem. 87 (3), 1582–1589.
Fan, R., Vermesh, O., Srivastava, A., Yen, B.K.H., Qin, L., Ahmad, H., Kwong, G.A., Liu, C.-C., Gould, J., Hood, L., Heath, J.R., 2008. Integrated barcode chips for rapid, multiplexed analysis of proteins in microliter quantities of blood. Nat. Biotech. 26 (12), 1373–1378.

Fu, Q., Zhu, J., Van Eyk, J.E., 2010. Comparison of multiplex immunoassay platforms. Clin. Chem. 56 (2), 314–318.
Ghodbane, M., Stucky, E.C., Maguire, T.J., Schloss, R.S., Shreiber, D.I., Zahn, J.D., Yarmush, M.L., 2015. Development and validation of a microfluidic immunoassay capable of multiplexing parallel samples in microliter volumes. Lab Chip 15 (15), 3211–3221.
He, B., Son, S.J., Lee, S.B., 2007. Suspension array with shape-coded silica nanotubes for multiplexed immunoassays. Anal. Chem. 79 (14), 5257–5263.
He, Q., Liu, Y., He, Y., Zhu, L., Zhang, Y., Shen, Z., 2016. Digital barcodes of suspension array using laser induced breakdown spectroscopy. Sci. Rep. 6, 36511.
Houser, B., 2012. Bio-Rad's Bio-Plex® suspension array system, xMAP technology overview. Arch. Physiol. Biochem. 118 (4), 192–196.
Hu, M., Yan, J., He, Y., Lu, H., Weng, L., Song, S., Fan, C., Wang, L., 2010. Ultrasensitive, multiplexed detection of cancer biomarkers directly in serum by using a quantum dot-based microfluidic protein chip. ACS Nano 4 (1), 488–494.
Hu, R., Liu, T., Zhang, X.-B., Yang, Y., Chen, T., Wu, C., Liu, Y., Zhu, G., Huan, S., Fu, T., Tan, W., 2015. DLISA: a DNAzyme-Based ELISA for protein enzyme-free immunoassay of multiple analytes. Anal. Chem. 87 (15), 7746–7753.
Jiang, L., Shen, Y., Zheng, K., Li, J., 2014. Rapid and multiplex microRNA detection on graphically encoded silica suspension array. Biosens. Bioelectron. 61, 222–226.
Juncker, D., Bergeron, S., Laforte, V., Li, H., 2014. Cross-reactivity in antibody microarrays and multiplexed sandwich assays: shedding light on the dark side of multiplexing. Curr. Opin. Chem. Biol. 18, 29–37.
Kim, S.-H., Shim, J.W., Yang, S.-M., 2011. Microfluidic multicolor encoding of microspheres with nanoscopic surface complexity for multiplex immunoassays. Angew. Chem. Int. Ed. 50 (5), 1171–1174.
Kingsmore, S.F., 2006. Multiplexed protein measurement: technologies and applications of protein and antibody arrays. Nat. Rev. Drug Discov. 5 (4), 310–321.
Krishnan, V.V., Selvan, S.R., Parameswaran, N., Venkateswaran, N., Luciw, P.A., Venkateswaran, K.S., 2018. Proteomic profiles by multiplex microsphere suspension array. J. Immunol. Methods 461, 1–14.
Le Goff, G.C., Srinivas, R.L., Hill, W.A., Doyle, P.S., 2015. Hydrogel microparticles for biosensing. Eur. Polym. J. 72, 386–412.
Lee, H., Kim, J., Kim, H., Kim, J., Kwon, S., 2010. Colour-barcoded magnetic microparticles for multiplexed bioassays. Nat. Mater. 9 (9), 745–749.
Leng, Y., Sun, K., Chen, X., Li, W., 2015. Suspension arrays based on nanoparticle-encoded microspheres for high-throughput multiplexed detection. Chem. Soc. Rev. 44 (15), 5552–5595.
Mathur, A., Kelso, D.M., 2010. Multispectral image analysis of binary encoded microspheres for highly multiplexed suspension arrays. Cytom. Part A 77A (4), 356–365.
Mora, J., Chunyk, A.G., Dysinger, M., Purushothama, S., Ricks, C., Österlund, K., Theobald, V., 2014. Next generation ligand binding assays—review of emerging technologies' capabilities to enhance throughput and multiplexing. AAPS J. 16 (6), 1175–1184.
Piemonti, L., Everly, M.J., Maffi, P., Scavini, M., Poli, F., Nano, R., Cardillo, M., Melzi, R., Mercalli, A., Sordi, V., Lampasona, V., Espadas de Arias, A., Scalamogna, M., Bosi, E., Bonifacio, E., Secchi, A., Terasaki, P.I., 2013. Alloantibody and autoantibody monitoring predicts islet transplantation outcome in human type 1 diabetes. Diabetes 62 (5), 1656–1664.
Pregibon, D.C., Toner, M., Doyle, P.S., 2007. Multifunctional encoded particles for high-throughput biomolecule analysis. Science 315 (5817), 1393–1396.
Rekers, N.V., von Herrath, M.G., Wesley, J.D., 2015. Immunotherapies and immune biomarkers in Type 1 diabetes: a partnership for success. Clin. Immunol. 161 (1), 37–43.
Spriggs, F.P., Zhong, Z.D., Safavi, A., Jani, D., Dontha, N., Kant, A., Ly, J., Brilando, L., Österlund, K., Rouleau, N., Fischer, S.K., Boissonneault, M., Ray, C., 2012. Ligand binding assays in the 21st century laboratory: platforms. AAPS J. 14 (1), 113–118.
Stoeva, S.I., Lee, J.-S., Smith, J.E., Rosen, S.T., Mirkin, C.A., 2006. Multiplexed detection of protein cancer markers with biobarcoded nanoparticle probes. J. Am. Chem. Soc. 128 (26), 8378–8379.
Tighe, P.J., Ryder, R.R., Todd, I., Fairclough, L.C., 2015. ELISA in the multiplex era: potentials and pitfalls. Proteom. – Clin. Appl. 9 (3–4), 406–422.
Tu, J., Bennett, P., 2017. Parallelism experiments to evaluate matrix effects, selectivity and sensitivity in ligand-binding assay method development: pros and cons. 9 (14), 1107–1122.
Vansant, E.F., Van Der Voort, P., Vrancken, K.C., 1995. Characterization and Chemical Modification of the Silica Surface.
Waterboer, T., Sehr, P., Pawlita, M., 2006. Suppression of non-specific binding in serological Luminex assays. J. Immunol. Methods 309 (1–2), 200–204.
Wenzlau, J.M., Juhl, K., Yu, L., Moua, O., Sarkar, S.A., Gottlieb, P., Rewers, M., Eisenbarth, G.S., Jensen, J., Davidson, H.W., Hutton, J.C., 2007. The cation efflux transporter ZnT8 (Slc30A8) is a major autoantigen in human type 1 diabetes. Proc. Natl. Acad. Sci. USA 104 (43), 17040–17045.
Xu, W., Chen, C., Ma, X., Yuan, L., Liu, S., Zheng, K., Li, J., 2017. Digitally encoded silica microparticles for multiplexed nucleic acid detection. Chem. Commun. 53 (43), 5866–5869.
Yamanishi, C.D., Chiu, J.H.-C., Takayama, S., 2015. Systems for multiplexing homogeneous immunoassays. Bioanalysis 7 (12), 1545–1556.
Yeung, D., Ciotti, S., Purushothama, S., Gharakhani, E., Kuesters, G., Schlain, B., Shen, C., Donaldson, D., Mikulskis, A., 2016. Evaluation of highly sensitive immunoassay technologies for quantitative measurements of sub-pg/ml levels of cytokines in human serum. J. Immunol. Methods 437, 53–63.
Yurkovetsky, Z.R., Kirkwood, J.M., Edington, H.D., Marrangoni, A.M., Velikokhatnaya, L., Winans, M.T., Gorelik, E., Lokshin, A.E., 2007. Multiplex analysis of serum cytokines in melanoma patients treated with interferon-α2b. Clin. Cancer Res. 13 (8), 2422–2428.
Zhang, B., Kumar, R.B., Dai, H., Feldman, B.J., 2014. A plasmonic chip for biomarker discovery and diagnosis of type 1 diabetes. Nat. Med. 20 (8), 948–953.
Zhang, F., Shi, Q., Zhang, Y., Shi, Y., Ding, K., Zhao, D., Stucky, G.D., 2011. Fluorescence upconversion microbarcodes for multiplexed biological detection: nucleic acid encoding. Adv. Mater. 23 (33), 3775–3779.
Zhao, X., Modur, V., Carayannopoulos, L.N., Laterza, O.F., 2015. Biomarkers in pharmaceutical research. Clin. Chem. 61 (11), 1343–1353.
Zhao, Y., Zhao, X., Sun, C., Li, J., Zhu, R., Gu, Z., 2008. Encoded silica colloidal crystal beads as supports for potential multiplex immunoassay. Anal. Chem. 80 (5), 1598–1605.
Zong, C., Wu, J., Wang, C., Ju, H., Yan, F., 2012. Chemiluminescence imaging immunoassay of multiple tumor markers for cancer screening. Anal. Chem. 84 (5), 2410–2415.